PHYSICAL REVIEW D VOLUME 12, NUMBER 11 1 DECEMBER 1975

# Neutrino (antineutrino) disintegration of the deuteron and the structure of the neutral weak current*

Ahmed Ali†
*Departamento de Física, Centro de Investigación y de Estudios Avanzados del Instituto Politecnico Nacional, Apdo. Postal 14-740, México 14, D.F.*
*and Physics Department, Stevens Institute of Technology, Hoboken, New Jersey 07030*

C. A. Dominguez‡
*Departamento de Física, Centro de Investigación y de Estudios Avanzados Instituto Politecnico Nacional, Apdo. Postal 14-740, México 14, D.F.*
(Received 5 May 1975)

We study the neutrino (antineutrino) disintegration of the deuteron with the view of determining the isospin and Lorentz character of the neutral weak current. Neutrino-induced transition rates between the ${}^3S\rightarrow{}^1S$, ${}^3S\rightarrow{}^1P$, and ${}^3S\rightarrow{}^3P$ of the neutron-proton system are derived for the most general form of the neutral weak current, valid up to intermediate neutrino energies (0–500 MeV). Explicit results are presented for the Weinberg-Salam model, the Bég-Zee model, and the case of an isoscalar neutral weak current. It is argued that this process can be, in principle, used to distinguish between the various assignments of the Lorentz and isospin properties of the hadronic neutral weak current.

## I. INTRODUCTION

The recent results of the Harvard-Pennsylvania-Wisconsin[1] collaboration for the neutral-current-induced inclusive processes indicate that the Lorentz character of the hadronic neutral weak current may not be the familiar $V-A$ of the charged weak currents. This has encouraged a more systematic study of the nature of neutral weak currents.[2] The problem of understanding the properties of the neutral weak currents is important in its own right, but it can also be used to test the gauge theory strategy where these currents have definite isospin and Lorentz properties. Naturally, this question can only be decided by measuring the different pieces of the hadronic weak currents and their relative contributions in a number of elementary particle and nuclear transitions. In this paper, we advocate the neutrino (antineutrino) disintegration of the deuteron as a possible mechanism to determine the detailed structure of the hadronic neutral weak current.

Our strategy is to write down the most general form of the neutral weak current, having arbitrary isospin and Lorentz properties but compatible with the observed helicities of the neutrinos, and to study the relative contribution of the different pieces of this current to the process under consideration, namely,

$$\nu(\bar{\nu})+d\rightarrow \nu(\bar{\nu})+n+p\,. \tag{1.1}$$

To that end, we calculate the differential and total cross sections for the neutrino-induced transitions ${}^3S\rightarrow{}^1S$, ${}^3S\rightarrow{}^1P$, and ${}^3S\rightarrow{}^3P$ of the neutron-proton system. Obviously, our results apply only up to intermediate neutrino energies where the higher partial waves can be safely ignored. We derive a threshold theorem which states that at and near the threshold only a Gamow-Teller (GT) type transition is possible between nondiagonal nuclear levels. In the case of the deuteron, this is caused by the isovector part of the axial-vector current, $A_i^3$. Away from the threshold, one has to study the other forbidden transitions which, obviously, are not appreciable unless the incident neutrino energy is large. The transition ${}^3S\rightarrow{}^1P$ is a pure isoscalar transition brought about by the isoscalar time component of the axial-vector current $A_0^{(0)}$, and the isoscalar part of the spatial vector current $V_i^{(0)}$, whereas the ${}^3S\rightarrow{}^3P$ is a pure isovector transition brought about by $A_i^{(3)}$ and $V_0^{(3)}$. These transitions have different energy dependence and one can, in principle, distinguish between them. Our conclusion is that at reactor energies ($E_{\bar{\nu}}\leqslant 10$ MeV), one can distinguish between the following possibilities: (i) The neutral weak current has a component that transforms like $A_i^{(3)}$; (ii) it may have arbitrary structure but not an $A_i^{(3)}$ piece.

Case (i) pertains to, for example, the Weinberg-Salam model.[3] The reason is that at these energies only models of type (i) can induce the allowed GT transitions ${}^3S\rightarrow{}^1S$, and both the ${}^3S\rightarrow{}^1P$ and ${}^3S\rightarrow{}^3P$ transitions which can be caused by models of type (ii) have rates that are well below the experimental resolution. However, at Los Alamos Meson Physics Facility (LAMPF) energies[4] ($E_\nu\leqslant 53$ MeV) it is possible to differentiate between (i) and (iii) a purely vector-isovector neutral hadronic weak current and (iv) a purely isoscalar neutral weak current.

Case (iii) pertains to, for example, the Bég-Zee model[5] whereas (iv) is advocated by Sakurai.[6]

To quantify our conclusions, we have presented our results for the Weinberg-Salam model, the Bég-Zee model, and the case of an isoscalar current. The results in the last case are arbitrary because of the arbitrary normalization of the isoscalar current. We have explained this in detail in the text. Results for the Weinberg-Salam model are presented separately for the reactor and LAMPF energies, which are independent of the Weinberg angle, $\theta_W$, as well as for the intermediate energies ($100 \leqslant E_{\nu,\bar{\nu}} \leqslant 600$ MeV) where they depend (~10%) on this angle. Results for the latter are given for $\sin^2\theta_W = 0.3$ and 0.4. In the Bég-Zee model we have fixed the mixing angle, $\theta_\xi$, from data on neutral weak current inclusive semileptonic processes and the results are given only for one value of $\theta_\xi$. We remark that process (1) becomes visible in this model ($\sigma \sim 10^{-45}$ cm$^2$) at a neutrino energy ($E_\nu = 30$ MeV) through the vector-isovector component in the neutral weak current.

This paper is organized as follows: Section II contains a derivation of the threshold theorem, an analysis of the neutral-current form factors, and the derivation of the differential (in reduced nucleon energy, $E_k$) and total cross sections for the various transitions. Section III contains the results that we obtain in the various models and are summarized through graphs.

## II. DERIVATION OF TRANSITION RATES

### A. Kinematics and approximations[7]

The kinematics of the process (1) is shown in Fig. 1. The most general form of the effective semileptonic interaction (for $q^2 \ll m_Z^{\,2}$) is

$$\mathcal{L}^{\text{effective}} = \frac{igg'}{m_Z^{\,2}}[\bar{\nu}_e\gamma_\mu(1+\gamma_5)\nu_e + \nu_e \to \nu_\mu]J^{\mu Z}(x), \tag{2.1}$$

where the couplings $g$ and $g'$ have their origin in the interaction of the leptonic and hadronic neutral weak currents to the neutral weak boson,

$$\mathcal{L}^{\text{leptonic}} = g j_\mu^{\text{leptonic}} Z^\mu(x), \tag{2.2}$$

$$\mathcal{L}^{\text{hadronic}} = g' J_\mu^Z Z^\mu(x) \tag{2.3}$$

and by $j_\mu^{\text{leptonic}}$ we mean the quantity in square brackets in (2.1). One can convince oneself that if the present helicities of the neutrinos are assumed not to flip in the neutral-current processes, then the most general Lorentz structure of the hadronic neutral weak current is a linear combination of vector and axial-vector parts:

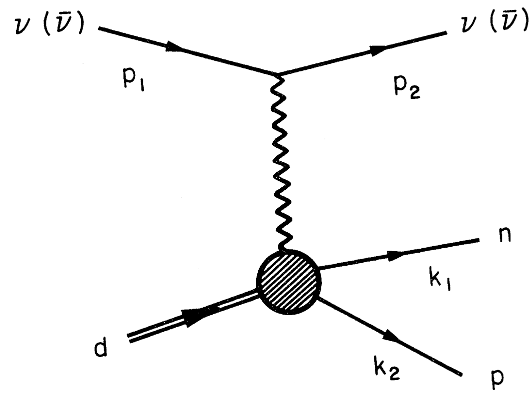


FIG. 1. Feynman diagram for the neutrino (antineutrino) disintegration of the deuteron.

$$J_\mu^Z(x) = V_\mu^Z(x) + \lambda A_\mu^Z(x). \tag{2.4}$$

We further introduce the isospin decomposition of the vector and axial-vector currents

$$\begin{aligned} V_\mu^Z(x) &= a_1 V_\mu^{(3)}(x) + a_3 V_\mu^{(0)}(x), \\ A_\mu^Z(x) &= a_2 A_\mu^{(3)}(x) + a_4 A_\mu^{(0)}(x), \end{aligned} \tag{2.5}$$

where the superscripts (3) and (0) represent the third component of an isovector and the isoscalar part, respectively. The interaction (2.1) leads to the following transition amplitude for the antineutrino disintegration of the deuteron:

$$T = i(2\pi)^4\delta^4(p_1 + m_D - p_2 - k_1 - k_2)\tilde{T}, \tag{2.6}$$

where

$$\begin{aligned} \tilde{T} = &\frac{iG_F}{\sqrt{2}\,(2\pi)^3}\bar{v}_\nu(p_1)\gamma_\mu(1-\gamma_5)v_\nu(p_2) \\ &\times\langle n(k_1)p(k_2)|J^{\mu Z}(0)|n(k_1')p(k_2'),{}^3S\rangle, \end{aligned} \tag{2.7}$$

$m_d$ is the mass of the deuteron, and

$$G_F = \frac{\sqrt{2}\,gg'}{m_Z^{\,2}}$$

is the Fermi coupling constant.

The amplitude for the neutrino disintegration of the deuteron is obtained from (2.7) by changing the spinors

$$\bar{v}_\nu(p_1) \to \bar{u}_\nu(p_2),$$
$$v_\nu(p_2) \to u_\nu(p_1).$$

In using Eq. (2.6) we shall make the following assumptions[8]:

i. The neutron and proton in the deuteron target are taken to be at rest and the deuteron to be a pure $^3S$ state of the ($n$-$p$) system. Nucleons in the final state are treated nonrelativistically in the sense that only leading terms in $q/m_N$, $k_1/m_N$, and $k_2/m_N$ are retained in the expansion of the matrix element (2.7). (The various momenta are defined through Fig. 1.)

ii. The independent-particle approximation states that the neutrino (antineutrino) is scattered elastically from each nucleon independently. In other words, the nuclear hadronic current density, $J_\mu^{\text{nuclear}}(x)$, is

$$J_\mu^{\text{nuclear}}(x)=\sum_{(\vec{p}\,'\sigma'\rho')}\sum_{(\vec{p}\sigma\rho)} a^\dagger_{(\vec{p}\,'\sigma'\rho')} \times\langle \vec{p}\,'\sigma'\rho'|J_\mu^Z(x)|\vec{p}\sigma\rho\rangle\, a_{(\vec{p}\sigma\rho)}\,,$$

where $(\vec{p}\sigma\rho)$ are a complete set of momentum, spin, and isospin quantum numbers for a nucleon. $a^\dagger, a$ are creation and annihilation operators in nuclear Hilbert space. The nucleons are treated on the mass shell. This introduces an additional approximation as the nucleons are bound in the deuteron and one expects an off-mass-shell effect for scattering due to bound nucleons. Also, because the system is described in terms of nucleon coordinates alone, no attempt is made to introduce meson-exchange effects either in the initial or final state.

iii. Nuclear physics effects are incorporated by assuming nuclear wave functions for the ground state and the excited states of the $(n$-$p)$ system. The effective-range approximation is used to determine the radial nuclear wave functions.

### B. Nucleon form factors of the neutral hadronic weak current

We write the most general form of the single nucleon matrix element of the neutral weak current as

$$\langle N(k)|J_\mu^Z(0)|N(k')\rangle=\frac{1}{(2\pi)^3}\left(\frac{m_N}{k_0}\right)^{1/2}\bar{u}_N(k)\,\Gamma_\mu^Z u_N(k')\,, \tag{2.8}$$

where

$$\Gamma_\mu^Z=\left[F_1^V(q^2)\gamma_\mu+i\sigma_{\mu\nu}(k-k')^\nu\frac{F_2^V(q^2)}{m_N}+(k-k')_\mu\frac{F_3^V(q^2)}{m_N}\right] +\lambda\left[\gamma_\mu\gamma_5F_1^A(q^2)+(k-k')_\mu\gamma_5F_P^A(q^2) +\gamma_5(k_1+k_2)_\mu\frac{F_3^A(q^2)}{m_N}\right]. \tag{2.9}$$

Note that all $F_i^{V,A}(q^2)$ are matrices in isospin space. These form factors are analyzed in the same way as is done for the charged weak current case. We write down the constraints on these form factors which come from the various symmetry considerations.

(i) The conserved-vector-current (CVC) hypothesis leads to $F_3^V(q^2)=0$.

(ii) Time-reversal invariance leads to the relative reality of all the form factors $F_i^{V,A}(q^2)$.

(iii) The absence of second-class currents demands $F_3^A(q^2)=0$.

(iv) $F_P^A(q^2)$: If $A_\mu(x)$ has an isovector piece then the hypothesis of partial conservation of the axial-vector current (PCAC) leads to a relation between the isovector parts of $F_P^A(q^2)$ and $F_1^A(q^2)$, namely the Goldberger-Treiman[9] relation:

$$F_P^{A(3)}(q^2)=2m_NF_1^{A(3)}(q^2)/(q^2+m_\pi^{\,2})\,. \tag{2.10}$$

However, the same statement is not true for the isoscalar part of $F_P^A(q^2)$, because strong interactions appear to be approximately $SU(2)\otimes SU(2)$-symmetric but not $U(2)\otimes U(2)$-symmetric. For elastic neutrino-nucleon scattering this term will be absent because of the factor $(k-k')_\mu$ which multiplies $F_P^A(q^2)$ with the lepton mass in the amplitude. For the neutrino-nucleus scattering this term gives a contribution proportional to $m_NE_K/(q^2+m_\pi^{\,2})$ and can be large.

Next, we introduce the isovector and isoscalar form factors in an obvious notation

$$F_i^{V,A}(q^2)=F_i^{(3)V,A}(q^2)\tau_3+F_i^{(0)V,A}(q^2)I\,. \tag{2.11}$$

Isospin rotation then simply relates $F_1^{(3)V}$ and $F_1^{(0)V}$ to the isovector and isoscalar Dirac form factors of the nucleon. $F_2^{(3)V}$ and $F_2^{(0)V}$ are likewise related to the corresponding Pauli form factors. $F_1^{(3)A}$ can be related to the $F_1^{(\pm)A}$, the isovector form factors for the charged weak currents, which are measured in the processes

$$\begin{pmatrix}\nu\\ \bar\nu\end{pmatrix}+\begin{pmatrix}n\\ p\end{pmatrix}\to\begin{pmatrix}\mu^-\\ \mu^+\end{pmatrix}+\begin{pmatrix}p\\ n\end{pmatrix}$$

and are also known. This leaves the isoscalar axial-vector form factors $F_1^{(0)A}(q^2)$ and $F_p^{(0)}(q^2)$ to be determined from the experiments involving purely neutral weak current transitions. The identification (modulo normalization) of the form factors $F_1^{V,A}$, etc., with the already measured form factors also fixes their $q^2$ dependence. Obviously, for the two unrelated form factors $F_1^{(0)A}(q^2)$ and $F_P^{(0)}(q^2)$ one has to make additional assumptions. However, we have neglected all $q^2$ dependence of the form factors in the energy region in which we are interested.

### C. Threshold theorem for the deuteron[10]

At threshold ($E_\nu=2.225$ MeV $=E_b=$binding energy of the deuteron), the momentum transfer to a nucleon is zero; hence for either nucleon

$$\langle N(k)|\, V_0\, |N(k')\rangle = \frac{i}{(2\pi)^3} u_N^*(k) F_1^V u_N(k')\,,$$
$$\langle N(k)|\, V_i\, |N(k')\rangle = \langle N(k)|A_0|N(k')\rangle = 0\,, \qquad (2.12)$$
$$\langle N(k)|\, A_i\, |N(k')\rangle = \frac{i}{(2\pi)^3} u_N^*(k)\sigma_i^N F_1^A u_N(k')\,.$$

However, CVC states that [$|n(k_1'), p(k_2'), {}^3S\rangle$ is the initial deuteron state]

$$\langle n(k_1)p(k_2)|\, V_0\, |n(k_1')p(k_2'), {}^3S\rangle = \frac{q_i}{q_0}\langle n(k_1)p(k_2)|\, V_i\, |n(k_1')p(k_2'), {}^3S\rangle\,, \qquad (2.13)$$

and because at threshold $q_0 = E_b \neq 0$, only the axial-vector part of the neutral current will induce a transition. It is easy to see that only $A_i^{(3)}$ can cause a transition, as near the threshold only the isospin-flip and spin-flip ${}^3S \to {}^1S$ transition is important, i.e., an allowed Gamow-Teller transition. That this is a matter of general circumstance for the nuclear neutral weak transitions at the threshold is easy to establish. First note that at the threshold, the $S \to P$ transition is strictly forbidden. If the transition involved is $l \to l$ (where $l$ is any angular momentum state) then it can be caused only through $V_0$ and $A_i$. Now if the transition induces a change in energy ($\Delta E = E_{N^*} - E_N \neq 0$) then CVC forbids the transition induced by $V_0$. This, however, does not preclude the coherent scattering of neutrinos off nucleus at the threshold, for the simple reason that in such processes $q_0$ at the threshold is zero and the CVC argument (2.13) does not hold. This leaves only the transition induced by $A_i$. Which isotopic part of $A_i$ induces a transition is then determined by whether or not the isospin is flipped. In this sense ($\Delta E \neq 0$) transitions caused by $V_0$, $V_i$, and $A_0$ are all forbidden transitions and one can see that unless the energy of the neutrinos is very high, these transitions will not be visible with the present experimental resolution. This leads to the conclusion that nondiagonal (nondegenerate in energy) nuclear transitions can be experimentally studied (at reactor energies) *only* if there is an axial-vector part in the neutral weak current.

### D. Transition amplitudes

We derive the most general form of the transition amplitude for the process (1) with the assumptions listed in subsection B:

$$\begin{aligned}
M(\bar\nu) \simeq \frac{G_F}{\sqrt{2}\,(2\pi)^3}\int d^3x\, e^{i(\vec p_1 - \vec p_2)\cdot\vec x}\psi_f^*(r) \\
\times\Bigg\{ \bar\nu_e(p_1)\gamma_0(1+\gamma_5)\nu_e(p_2)\Bigg[2a_3F_1^{(0)V} + \tfrac{1}{2}\lambda a_2 F_1^{(3)A}\tau_3\left(\frac{1}{m_p}(\vec\sigma^S\cdot\vec k_2 + \vec\sigma^A\cdot\vec k_2) + \frac{1}{m_n}(\vec\sigma^S\cdot\vec k_1 - \vec\sigma^A\cdot\vec k_1)\right)\Bigg] \\
+ \tfrac{1}{2}\bar\nu_e(p)\gamma^i(1+\gamma_5)\nu_e(p')\Bigg[a_1F_1^{(3)V}\tau_3\left(\frac{k_{2i}}{m_p} - \frac{k_{1i}}{m_n}\right) + a_3F_1^{(0)V}\left(\frac{k_{2i}}{m_p} + \frac{k_{1i}}{m_n}\right) \\
- i\epsilon_{ijk}(a_1F_1^{(3)V}\tau_3 + 2a_1F_2^{(3)V}\tau_3 + a_3F_1^{(0)V} + 2a_3F_2^{(0)V})(\sigma_k^S + \sigma_k^A)\frac{k_{2j}}{m_p} \\
- i\epsilon_{ijk}(a_3F_1^{(0)V} + 2a_3F_2^{(0)V} - a_1F_1^{(3)V}\tau_3 - 2a_1F_2^{(3)V}\tau_3)(\sigma_k^S - \sigma_k^A)\frac{k_{1j}}{m_n} \\
+ 4\lambda(a_2\tau_3F_1^{(3)A}\sigma_i^A + a_4F_1^{(0)A}\sigma_i^S)\Bigg]\Bigg\}\psi_i(r)\,. \qquad (2.14)
\end{aligned}$$

$\psi_i(x)$, the deuteron wave function, and $\psi_f(x)$, the final-state ($n$-$p$) wave functions are taken from the nuclear physics studies of the neutron-proton system. All one has to do to calculate the various transition rates is to do a standard multipole analysis. One expands the exponential in terms of the basic multipole operators; as well, one keeps the nonleading terms in the hadronic current matrix element. One then uses the orthogonality relations between the various special functions to do the angular integrals. The radial integrals are evaluated by solving the radial Schrödinger equation for the ($n$-$p$) system. This involves assuming a potential. To determine the radial functions we have taken over, as such, the treatment of Bethe *et al.*[11] for the photomagnetic and photoelectric dissociation of the deuteron in the effective-range approximation. The results for the differential cross sections are listed below.

### E. Differential cross sections

*i.* $^3S\to{}^1S$

In this case we have

$$\frac{d\sigma}{dE_k}\begin{pmatrix}\nu\\ \bar\nu\end{pmatrix}=\frac{G^2}{12\pi^2}\frac{m^{3/2}E_k^{1/2}\gamma}{(mE_ka_S^2+1)}\frac{(|p_1|-E_d-E_k)^2}{(1-\gamma r_{0t})}\left(\frac{\gamma a_S-1}{\gamma^2+mE_k}\right)^2$$
$$\times\Big\{96|a_2\lambda F_1^{(3)A}|^2+\frac{4}{m^2}|a_1(F_1^{(3)V}+2F_2^{(3)V})|^2[|\vec p_1|^2+\tfrac{4}{3}|\vec p_1|(|\vec p_1|-E_d-E_k)+(|\vec p_1|-E_d-E_k)^2]$$
$$\mp\frac{32}{m_N}\mathrm{Re}[a_1a_2\lambda F_1^{(3)A}(F_1^{(3)V}+2F_2^{(3)V})](2|\vec p_1|-E_k-E_d)\Big\}. \tag{2.15}$$

*ii.* $^3S\to{}^1P$

In this case we have

$$\frac{d\sigma}{dE_k}\begin{pmatrix}\nu\\ \bar\nu\end{pmatrix}=\frac{8}{9}\frac{G^2}{\pi^2}\frac{(|\vec p_1|-E_d-E_k)^2m^{3/2}E_k^{5/2}\gamma}{(1-\gamma r_{0t})(\gamma^2+mE_k)^4}$$
$$\times\{|\lambda a_4F_1^{(0)A}|^2[\vec p_1^{\,2}+(|\vec p_1|-E_d-E_k)^2-\tfrac{1}{3}|\vec p_1|(|\vec p_1|-E_d-E_k)]$$
$$+2|a_3(F_1^{(0)V}+2F_2^{(0)V})|^2[\vec p_1^{\,2}+(|\vec p_1|-E_d-E_k)^2+\tfrac{2}{9}|\vec p_1|(|\vec p_1|-E_d-E_k)]\}. \tag{2.16}$$

*iii.* $^3S\to{}^3P$

In this case we have

$$\frac{d\sigma}{dE_k}\begin{pmatrix}\nu\\ \bar\nu\end{pmatrix}=\frac{8G^2}{3\pi^2}\frac{|a_1F_1^{(3)V}|^2m^{3/2}E_k^{5/2}\gamma}{(1-\gamma r_{0t})(\gamma^2+mE_k)^4}(|\vec p_1|-E_d-E_k)^2[\vec p_1^{\,2}+(|\vec p_1|-E_d-E_k)^2+\tfrac{2}{9}|\vec p_1|(|\vec p_1|-E_d-E_k)], \tag{2.17}$$

where

$$E_k=(\vec k_1-\vec k_2)^2/4m_N\,,\quad \gamma=(mE_d)^{1/2}, \tag{2.18}$$

and we have used the following expressions for the radial functions:

$$I_2^2\equiv\left|\int dr\,u_{0S}^*(r)u_g(r)\right|^2=\frac{2\gamma}{m_N(1-\gamma r_{0t})}\left[\frac{1}{(mE_ka_S^2+1)}\frac{\gamma a_S-1}{(E_d+E_k)}\right], \tag{2.19}$$

$$I_3^2\equiv\left|\int dr\,u_{1p}^*(r)u_g(r)r\right|^2\simeq\left[\frac{8E_k\sqrt{E_d}}{m_N^{5/2}(E_d+E_k)^4}\frac{1}{(1-\gamma r_{0t})}\right], \tag{2.20}$$

$$I_4^2\equiv\left|\int dr\,u_{2p}^*(r)u_g(r)r\right|^2\simeq I_3^2\,. \tag{2.21}$$

$a_S$ is the singlet scattering length and $r_{0t}$ is the triplet range. In deriving $I_3^2$ and $I_4^2$, we have ignored the final-state interaction. One expects an ~5% error in making this approximation.[7] This assumption, however, makes the calculation of the total cross section very simple.

### F. Total cross sections

*i.* $^3S\to{}^1S$

Here we have

$$\sigma\begin{pmatrix}\nu\\ \bar\nu\end{pmatrix}=A_1(\vec p_1^{\,2}Z_1-2|\vec p_1|Z_2+Z_3)+B_1\{\tfrac{10}{3}\vec p_1^{\,4}Z_1-10|\vec p_1|^3Z_2+[10\vec p_1^{\,2}-\tfrac{10}{3}|\vec p_1|E_d+(|\vec p_1|-E_d)^2]Z_3$$
$$-2[(|\vec p_1|-E_d)+\tfrac{5}{3}|\vec p_1|]Z_4+Z_5]\mp C_1[2\vec p_1^{\,3}Z_1-5\vec p_1^{\,2}Z_2+(4|\vec p_1|-E_d)Z_3-Z_4], \tag{2.22}$$

where

$$A_1=\frac{8G^2|a_2\lambda F_1^{(3)A}|^2\sqrt{E_d}\,(\gamma a_S-1)^2}{\pi^2(1-\gamma r_{0t})}, \tag{2.23a}$$

$$B_1 = \frac{1}{3\pi^2} G^2 \frac{|a_1(F_1^{(3)V} + 2F_2^{(3)V})|^2 \sqrt{E_d}\,(\gamma a_S - 1)^2}{m^2(1-\gamma r_{0t})}, \tag{2.23b}$$

$$C_1 = \frac{8}{3\pi^2} G^2 \,\mathrm{Re}[a_1 a_2 \lambda F_1^{(3)A}(F_1^{(3)V} + 2F_2^{(3)V})]\sqrt{E_d}\,\frac{(\gamma a_S - 1)^2}{m(1-\gamma r_{0t})}. \tag{2.24}$$

The various $Z_i$'s are functions of $E_k^{\max} = |\vec{p}_1| - E_d$ and are given in the Appendix.

*ii.* $^3S \to {}^1P$

Here we have

$$\sigma(\nu) = \sigma(\bar{\nu}) = A_2(\tfrac{5}{6}\vec{p}_1{}^4 Z_6 + \tfrac{5}{6}|\vec{p}_1|^3 Z_7 + \tfrac{6}{7}|\vec{p}_1|^2 Z_8 + \tfrac{11}{12}|\vec{p}_1| Z_9 + Z_{10})$$
$$+ B_2(\tfrac{10}{9}\vec{p}_1{}^4 Z_6 + \tfrac{10}{9}|\vec{p}_1|^3 Z_7 + \tfrac{23}{21}|\vec{p}_1|^2 Z_8 + \tfrac{19}{18}|\vec{p}_1| Z_9 + Z_{10}), \tag{2.25}$$

where

$$A_2 = \frac{8G^2|\lambda a_4 F_1^{(0)A}|^2\sqrt{E_d}}{9\pi^2(1-\sqrt{mE_d}\,r_{0t})m_N{}^2}, \tag{2.26}$$

$$B_2 = \frac{16G^2 a_3{}^2 |F_1^{(0)V} + 2F_2^{(0)V}|^2\sqrt{E_d}}{9\pi^2(1-\sqrt{mE_d}\,r_{0t})m_N{}^2}. \tag{2.27}$$

*iii.* $^3S \to {}^3P$

Here we have

$$\sigma(\nu) = \sigma(\bar{\nu}) = A_3(\tfrac{10}{9}\vec{p}_1{}^4 Z_6 + \tfrac{10}{9}|\vec{p}_1|^3 Z_7 + \tfrac{23}{21}|\vec{p}_1|^2 Z_8 + \tfrac{19}{18}|\vec{p}_1| Z_9 + Z_{10}), \tag{2.28}$$

where

$$A_3 = \frac{8G^2|a_1 F_1^{(3)V}|^2\sqrt{E_d}}{3\pi^2 m_N{}^2[1-(m_N E_d)^{1/2} r_{0t})}. \tag{2.29}$$

## III. RESULTS

We present the results for the following three models:

(i) the Weinberg-Salam model;
(ii) the Bég-Zee model;
(iii) the isoscalar neutral current model.

The results for the total cross sections are summarized through the various graphs.

*i. Weinberg-Salam model.*[3] The hadronic neutral weak current in this model is given by the expression

$$j_\mu^Z = (V^{(3)} - A^{(3)})_\mu - 2\sin^2\theta_W \left(V^{(3)} + \frac{1}{\sqrt{3}} V^{(8)}\right)_\mu, \tag{3.1}$$

and has the $V-A$ structure as is the case for the charged hadronic weak currents. The angle $\theta_W$ is defined as

$$\cos^2\theta_W = \frac{m_W{}^2}{m_Z{}^2}, \tag{3.2}$$

where $m_W$ is the mass of the charged weak boson $W^\pm$.

In terms of our parameters the model is characterized by

$$\begin{aligned} a_1 &= (1-2\sin^2\theta_W), \\ a_3 &= -2\sin^2\theta_W, \\ a_2 &= -1, \\ a_4 &= 0 \text{ (no isoscalar axial-vector part).} \end{aligned} \tag{3.3}$$

Total cross sections are shown in Figs. 2 and 3. We remark that up to the energies we have considered ($E_{\nu,\bar{\nu}} = 500$ MeV) it is the $^3S \to {}^1S$ transition that dominates. Figure 2 is valid for the reactor and LAMPF energies and is almost independent of the Weinberg angle. Figure 3 shows the total cross section from LAMPF energies up to $E_{\nu,\bar{\nu}} = 500$ MeV and depends on the mixing angle $\theta_W$. The curve in Fig. 2 is drawn for $\sin^2\theta_W = 0.3$ which comes from a theoretical fit to the data on inclusive neutrino-nucleon neutral-current processes.[12] However, the value $\sin^2\theta_W = 0.4$ is also not ruled out.[1] In Fig. 3 we have shown the dependence of the total cross section on $\theta_W$ for the two values of $\theta_W$, $\sin^2\theta_W = 0.3$ and $\sin^2\theta_W = 0.4$.

The gross features in this model are that $\sigma_\nu$ and $\sigma_{\bar{\nu}}$ are almost equal, and independent of the Weinberg angle, up to LAMPF energies. In the intermediate energy region both $\sigma_\nu$ and $\sigma_{\bar{\nu}}$ depend on the Weinberg angle and are in general different except,

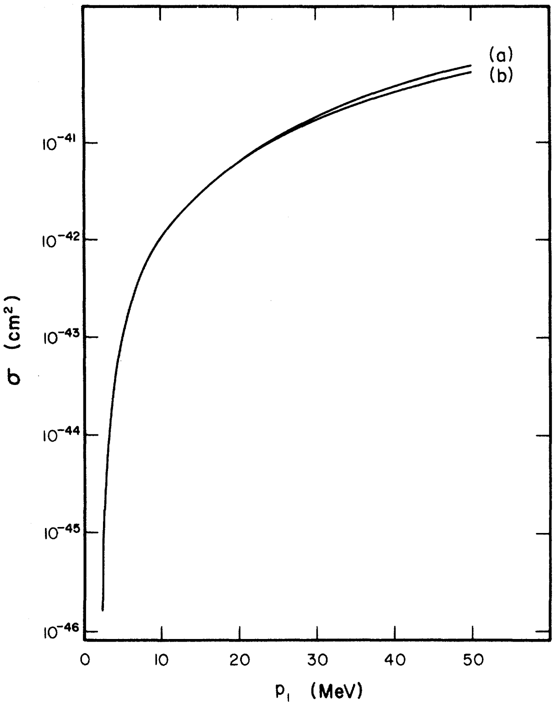


FIG. 2. Total cross section for the neutrino (a) and (b) disintegration of the deuteron plotted versus the incoming antineutrino energy, up to LAMPF energies, for the Weinberg-Salam model. The curves are drawn for $\sin^2\theta_W = 0.3$.

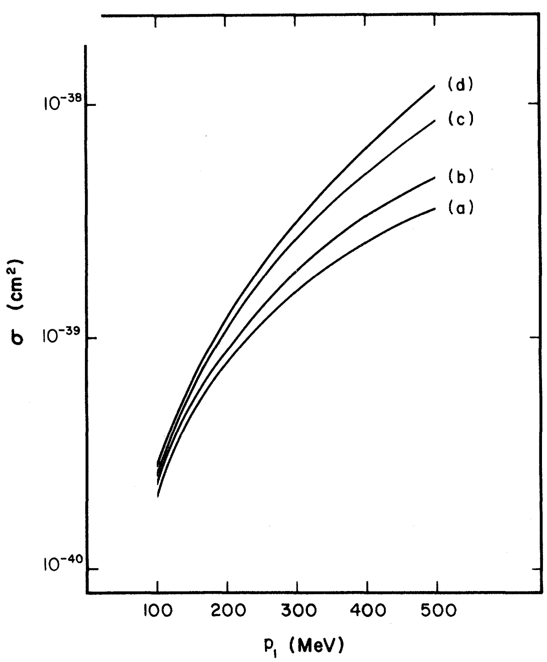


FIG. 3. Dependence of $\sigma_\nu$ and $\sigma_{\bar{\nu}}$ on the Weinberg angle $\theta_W$, for the $\nu(\bar{\nu})$ energy region 50 MeV $\leq |p_1| \leq$ 500 MeV. (a) $\sigma_{\bar{\nu}}$ for $\sin^2\theta_W = 0.3$; (b) $\sigma_{\bar{\nu}}$ for $\sin^2\theta_W = 0.4$; (c) $\sigma_\nu$ for $\sin^2\theta_W = 0.4$; (d) $\sigma_\nu$ for $\sin^2\theta_W = 0.3$.

of course, for $\sin^2\theta_W = 0.5$, where they are equal. Finally for models in which $j_\lambda^{\text{neutral}} = x j_\lambda^{\text{neutral}}$ (Salam-Weinberg), all the cross sections will be scaled uniformly by the scale factor $x^2$.

*ii. Bêg-Zee model.*[5] This model has the distinct feature of having a purely vector neutral weak current. The hadronic weak current has the form

$$j_\mu^Z = 2\frac{\sin^2\xi}{\cos^4\xi}(1 - 2\sin^2\xi)V_\mu^{(3)} - \frac{4}{\sqrt{3}}\tan^4\xi\, V_\mu^{(8)}, \tag{3.4}$$

with

$$\tan\xi = \frac{m_W}{m_Z}. \tag{3.5}$$

The various parameters have the values

$$a_1 = 2R,$$

$$a_3 = -4\frac{\sin^2\xi}{1 - 2\sin^2\xi}R,$$

$$a_2 = a_4 = 0,$$

where

$$R = \frac{\sin^2\xi}{\cos^4\xi}(1 - 2\sin^2\xi).$$

The total cross sections are shown in Figs. 4 and 5. In presenting these results we have assumed $\sin^2\theta\xi = 0.3$, which is obtained from a fit

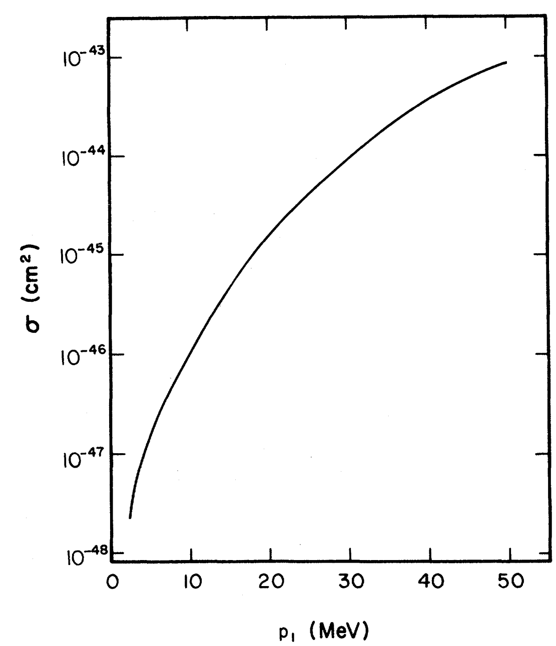


FIG. 4. Total cross section for the antineutrino (neutrino) disintegration of the deuteron up to LAMPF energies, in the Bêg-Zee model.

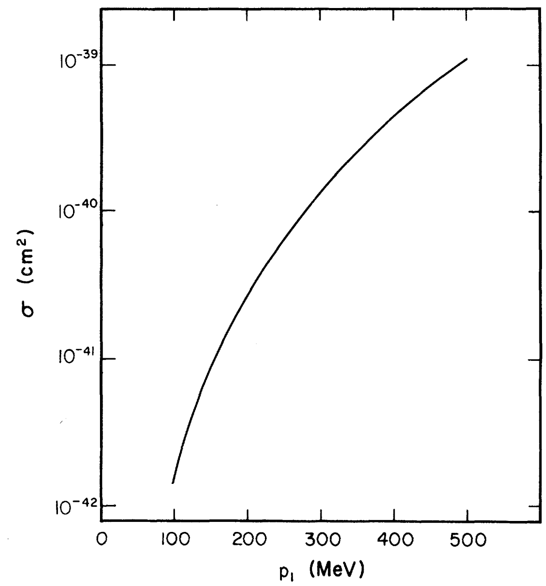


FIG. 5. Total cross section for the neutrino (antineutrino) disintegration of the deuteron for the energy region 50 MeV $\leq |p_1| \leq$ 500 MeV, in the Bég-Zee model.

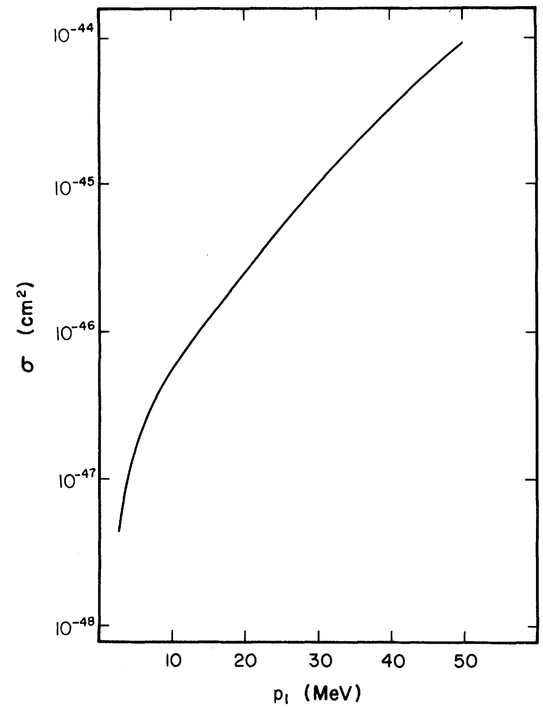


FIG. 6. Total cross section for the neutrino (antineutrino) disintegration of the deuteron in an isoscalar model, versus incoming neutrino (antineutrino) energies. The scale is arbitrary and we have chosen $|a_3|^2 = |\lambda a_4|^2 = 1$.

to the neutral-current-induced inclusive processes.[5] We note that the process (1) while invisible in this model at reactor energies ($\sigma \sim 10^{-46}$ cm$^2$) rises sharply and can be observed at LAMPF energies. The neutrino and antineutrino cross sections are, of course, equal.

*iii. Isoscalar neutral weak current.*[6] Results for the isoscalar model are shown in Fig. 6, where the scale depends upon the relative strength of the vector and the axial-vector parts. As pointed out earlier this can only be decided by data on purely neutral current processes. Pending such a determination, we have arbitrarily chosen $|a_3|^2 = |a_4\lambda|^2 = 1$ in (2.25) for the $^3S \rightarrow {}^1P$ transition ($^3S \rightarrow {}^1S$ and $^3S \rightarrow {}^3P$ are $\Delta I = 1$ transitions). The coupling constant $F_1^{(0)A}$ is taken from the quark-model result $F_1^{(0,S)A}/F_1^{(3)A} \sim \frac{3}{5}$. We note that the reaction (1) in this class of models is not visible up to the LAMPF energies.

Experimentally, Gurr *et al.*[13] have presented a new upper limit for the antineutrino disintegration of the deuteron at the reactor energies, which is six times the Weinberg-Salam model calculation, at a 3-standard-deviation level. They propose to rerun this experiment with improved neutron detection efficiency. A precise determination of the reaction rate can considerably reduce the scope of theoretical speculation, and would be very welcome.

## ACKNOWLEDGMENT

The major part of this work was done at the Stevens Institute of Technology, Hoboken, and it was completed at the Centro de Investigación del IPN, Mexico. One of us (C. A. D.) would like to acknowledge the hospitality of Professor Jeremy Bernstein and Professor M. A. B. Bég during his stay at the Stevens Institute of Technology and Rockefeller University. The other (A. A.) would like to acknowledge the hospitality extended to him at the Centro de Investigación del IPN, Mexico. We are very grateful to Professor M. A. B. Bég and Professor Jeremy Bernstein for their continued interest and guidance. One of us (C. A. D.) wishes to thank Dr. A. Zepeda for helpful discussions. Finally we are indebted to Professor L. Wolfenstein for calling our attention to a mistake present in the first version of this paper.

## APPENDIX

The following are the expressions for the functions $Z_i$ used in the text:

$$Z_1 = \frac{\sqrt{E_k}}{(bE_d - 1)(E_k + E_d)} + \tan^{-1}\left(\left(\frac{E_k}{E_d}\right)^{1/2}\right)\frac{(bE_d + 1)}{\sqrt{E_d}\,(bE_d - 1)^2} - \frac{2\sqrt{b}}{(bE_d - 1)^2}\tan^{-1}((E_k b)^{1/2}), \quad \text{(A1)}$$

$$Z_2=\frac{2}{\sqrt{b}\,(1-bE_d)}\tan^{-1}((E_kb)^{1/2}) -\frac{2\sqrt{E_d}}{(1-bE_d)}\tan^{-1}((E_k/E_d)^{1/2}), \tag{A2}$$

$$Z_3=2\left[\frac{\sqrt{E_k}}{b}-\frac{1}{b^{3/2}}\tan^{-1}((E_kb)^{1/2})\right], \tag{A3}$$

$$Z_4=\frac{2}{b}\left[\tfrac{1}{3}E_k^{3/2}-\frac{1}{b}E_k^{1/2}+\frac{1}{b^{3/2}}\tan^{-1}((E_kb)^{1/2})\right], \tag{A4}$$

$$Z_5=\frac{1}{b}\left(\tfrac{2}{5}E_k^{5/2}-Z_4\right), \tag{A5}$$

$$Z_6=-\frac{1}{(E_k+E_d)^3}\left(4E_k^{5/2}+\tfrac{20}{3}E_dE_k^{3/2}+\tfrac{10}{3}E_d^2E_k^{1/2}\right) +\frac{25}{12}\frac{E_d\sqrt{E_k}}{(E_d+E_k)^2}+\frac{15}{12}\frac{E_k^{3/2}}{(E_k+E_d)^2} +\frac{15}{12}\frac{1}{\sqrt{E_d}}\tan^{-1}((E_k/E_d)^{1/2}), \tag{A6}$$

$$Z_7=-\frac{12E_k^{5/2}}{(E_k+E_d)^2}-\frac{60E_dE_k^{3/2}}{(E_k+E_d)^2}+\frac{45E_d^2\sqrt{E_k}}{(E_k+E_d)^2} +\frac{45}{2}\frac{E_d\sqrt{E_k}}{(E_k+E_d)}+\tfrac{45}{2}\sqrt{E_d}\tan^{-1}\left(\left(\frac{E_k}{E_d}\right)^{1/2}\right), \tag{A7}$$

$$Z_8=\frac{1}{(E_k+E_d)}\left(\tfrac{14}{3}E_k^{5/2}-\tfrac{70}{3}E_dE_k^{3/2}-35E_k^{1/2}E_d^2\right) +35E_d^{3/2}\tan^{-1}\left(\left(\frac{E_k}{E_d}\right)^{1/2}\right), \tag{A8}$$

$$Z_9=-8\left[\tfrac{1}{5}E_k^{5/2}-\tfrac{1}{3}E_k^{3/2}E_d+E_d^2\sqrt{E_k} -E_d^{5/2}\tan^{-1}((E_k/E_d)^{1/2})\right], \tag{A9}$$

$$Z_{10}=\tfrac{2}{7}E_k^{7/2}, \tag{A10}$$

$$b=ma_S^2. \tag{A11}$$

In all the above equations $E_k=p_1-E_d$, i.e., the maximum available energy.

---

*Work supported in part by NSF and by CONACyT (Mexico).

†Work supported in part by NSF under Grant No. GP-36777.

‡Work supported in part by CONACyT (Mexico) under Contract No. 540.

[1]A. Rousset, in *Neutrinos—1974,* proceedings of the Fourth International Conference on Neutrino Physics and Astrophysics, Philadelphia, edited by C. Baltay (A. I. P., New York, 1974), p. 141.

[2]S. L. Adler, Phys. Rev. Lett. 33, 1511 (1974).

[3]A. Salam, in *Elementary Particle Theory: Relativistic Groups and Analyticity (Nobel Symposium No. 8),* edited by N. Svartholm (Almqvist and Wiksell, Stockholm, 1968), p. 367; S. Weinberg, Phys. Rev. Lett. 19, 1264 (1967); 27, 1688 (1971); Phys. Rev. D 5, 1412 (1972).

[4]R. L. Burman *et al.*, Los Alamos Report No. LA-4842-MS 1971 (unpublished).

[5]M. A. B. Bég and A. Zee, Phys. Rev. Lett. 30, 675 (1973); Phys. Rev. D 8, 1460 (1973).

[6]J. J. Sakurai, Phys. Rev. D 9, 250 (1974); in *Neutrinos—1974,* proceedings of the Fourth International Conference on Neutrino Physics and Astrophysics, Philadelphia, edited by C. Baltay (A. I. P., New York, 1974), p. 57.

[7]The neutrino disintrgration of deuteron has been studied quite extensively in the literature even before the advent of gauge Field theories, Yu. V. Gapanov and I. V. Tyutin, Zh. Eksp. Teor. Fiz. 47, 1826 (1964) [Sov. Phys.—JETP 20, 1231 (1965)], have evaluated the cross sections for the $^3S\rightarrow{}^1S$ and $^3S\rightarrow{}^1P$ transitions based on a Hamiltonian which is similar to the one we use. We believe there is an error in their expression for the differential cross section for the transition $^3S\rightarrow{}^1P$. Also their results are valid only up to reactor energies. There are additional terms which one has to consider if one wants to study the process (1) in the intermediate energy regions. See also T. Ahrens and T. P. Lang, Phys. Rev. C 3, 979 (1971); C. P. Frahm, Phys. Rev. D 3, 663 (1971) and references quoted therein. The observation that at low energies only the axial vector (Gamow-Teller) contributes to this reaction leaving no arbitrary parameter in the Weinberg-Salam model was pointed out by T. W. Donnelly, D. Hitlin, M. Schwartz, J. D. Walecka, and S. J. Weisner, Phys. Lett. 49B, 8 (1974). Our treatment differs from the existing ones in that (1) we have studied the entire energy spectrum up to 500 MeV, and (2) we emphasize the relative contribution of different pieces in the most general hadronic neutral weak current with the view of determining the Lorentz and isospin properties of such a current.

[8]The assumptions made here are familiar from electron-nucleus and charged weal current processes. Their effects in these processes have been studied in detail in the literature. For references and general approach to study nuclear transitions using weak currents see J. D. Walecka, in *Muon Physics,* edited by V. W. Hughes and C. S. Wu (Academic, New York, to be published).

[9]M. L. Goldberger and S. B. Treiman, Phys. Rev. 110, 1178 (1956).

[10]M. A. B. Bég (private communication). See also J. J. Sakurai and L. F. Urrutia, Phys. Rev. D 11, 159 (1975). We are not aware if the extension of the threshold theorem for the deuteron to the neutral-current-induced nondiagonal nuclear transitions exists in the literature.

[11]H. A. Bethe and C. Longmire, Phys. Rev. 76, 38 (1949); 77, 647 (1950).

[12]L. M. Sehgal, Phys. Lett. 48B, 133 (1974); E. A. Paschos and L. Wolfenstein, Phys. Rev. D 7, 91 (1973).

[13]H. Gurr, F. Reines, and H. W. Sobel, Phys. Rev. Lett. 33, 179 (1974).